Organic & Biomolecular Chemistry

Accepted Manuscript

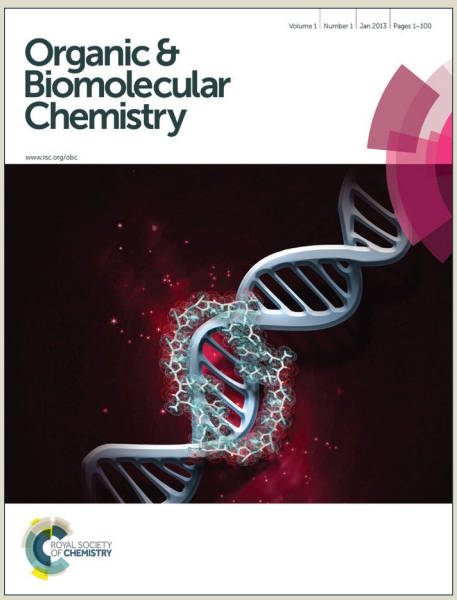

ROYAL SOCIETY OF CHEMISTRY

www.rsc.org/obc

Frontier Orbitals and Transition States in the Oxidation and Degradation of L-Ascorbic Acid: A DFT Study†

Shinichi Yamabe,[a]* Noriko Tsuchida,[b] Shoko Yamazaki[c] and Shigeyoshi Sakaki[a]

[a]*Fukui Institute for Fundamental Chemistry, Kyoto University, Takano-Nishihiraki-cho 34-4, Sakyou-ku, Kyoto 606-8103, Japan*

[b]*Department of Liberal Arts, Faculty of Medicine, Saitama Medical University, 38 Morohongo, Moroyama-machi, Iruma-gun, Saitama 350-0495 Japan*

[c]*Department of Chemistry, Nara University of Education, Takabatake-cho, Nara 630-8528, Japan*

email:yamabes@fukui.kyoto-u.ac.jp

Graphical Abstract

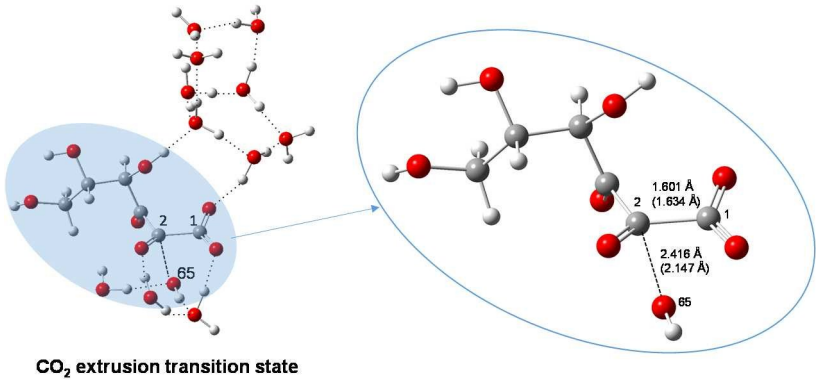

Abstract

DFT calculations were carried out to investigate reaction paths of L-ascorbic acid (AAH_2), hydroxyl radical and water clusters. Frontier-orbital analyses were also made to examine the regioselectivity of the OH· addition. Transition states of the electrolytic dissociation of AAH_2 and intermediate carboxylic acids were found to have very small activation energies through proton transfers along hydrogen bonds. The ionized species (anions) are subject to the electrophilic attack of OH·. The elementary processes of $AAH_2 \rightarrow AA^{\cdot -} \rightarrow$ dehydroascorbic

acid → diketogulonic acid → threonic, oxalic, xylonic and lyxonic acids were investigated and discussed. The processes involved in the conversion of dehydroascorbic acid into a bicyclic hemiketal were also examined as a side-chain participating reaction. The oxidation and degradation of vitamin C up to the threonic acid were described mainly as a donor (AAH_2) − acceptor ($OH\cdot$) reaction.

I. Introduction

Vitamin C is an important antioxidant in chemistry and biochemistry.[1] It was isolated first by Albert Szent-Gyorgyi from the adrenal cortex of cattle as a new carbohydrate derivative, and the molecular formula $C_6H_8O_6$ was proposed by him.[2] It was named huxuronic acid initially. However, the substance was found to possess strong antiscorbutic properties[3] and the name was changed to ascorbic acid (here called AAH_2).[4] AAH_2 was shown to be a powerful reducing agent and its structural formula was determined by Herbert et. al.[5] The first definite X-ray and neutron studies of AAH_2 were carried out by Hvoslef,[6] and the stereochemistry of AAH_2 was established as shown in the left of Scheme 1. ^{13}C NMR studies showed that the conformation in the crystal is the same as the dominant one in water solution.[7]

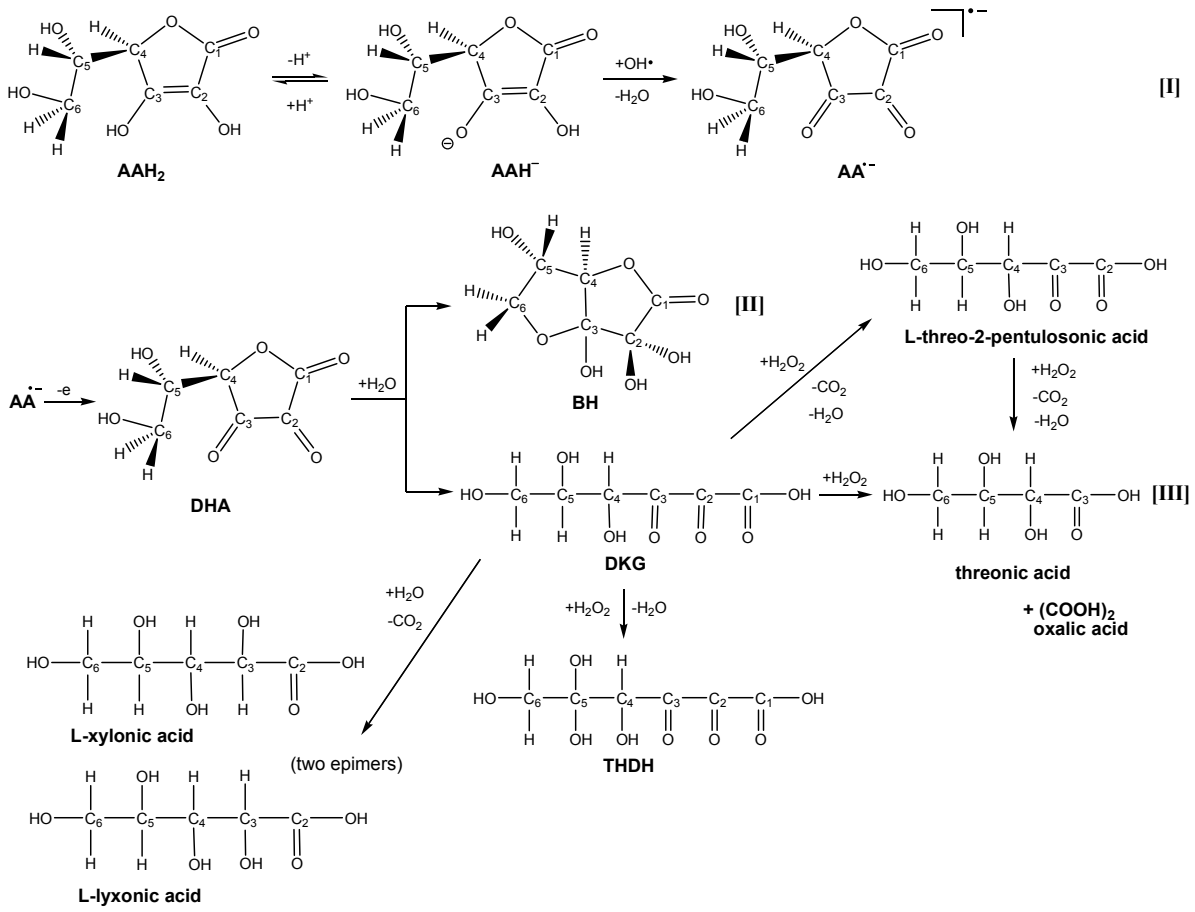

Scheme 1. Representative intermediates and products of the oxidative degradation of L-ascorbic acid (AAH_2) by hydroxyl radical and H_2O_2 in the water solution. Detailed definition of all species is described in Supplementary Information.

Many oxidations in physiological processes occur by the hydroxyl radical (HO·) causing damage to nucleic acids, proteins and lipids in human and other tissue. The hydroxyl radical is preferentially reduced to water leading to the oxidized form of ascorbate which is a more stable radical, less harmful to biological tissue than the radicals by which it is oxidized.[8] In 1960, during the enzymatic oxidation of AAH_2, a 1.7 Gauss ESR doublet signal was observed.[9] The radical was assigned to an ascorbate anion radical ($AA\cdot^-$ in Scheme 1) by a reaction between the ascorbic acid and hydroxyl radical using the in situ radiolysis-ESR method.[10] The electron paramagnetic resonance signal intensity of the $AA\cdot^-$ radical was shown to be an indicator of the degree of free radical processes taking place in chemical and

biochemical systems.[11]

The oxidation of AAH_2 leads to dehydroascorbic acid (DHA in Scheme 1) with the loss of hydrogens from carbons 2 and 3 via $AA^{\cdot -}$.[12,13] DHA undergoes the water addition in two ways. One is by formation of a bicyclic hemiketal (BH in Scheme 1) via the intramolecular ring closure.[14] The other is by formation of diketogulonic acid (DKG in Scheme 1) via the ring opening.[15] Further oxidation of DKG by H_2O_2 gives 4,5,5,6-tetrahydroxy-2,3-diketohexanoic acid (THDH in Scheme 1) as the first channel.[16] As the second channel, DKG reacts with H_2O_2 leading to trihydroxybutanoic acid (threonic acid in Scheme 1) along with oxalic acid.[17] The threonic acid of the L-isomer is known to be a metabolite of AAH_2.[18] The acid is also formed via L-threo-2-pentulosonic acid.[19] In the third channel, DKG in the rat kidney is converted to two pentonic acids (L-xylonic and L-lyxonic acids).[20]

Scheme 1 shows the main routes of the oxidative degradation of AAH_2 reported experimentally. Since AAH_2 is known to be oxidized to the threonic acid with pentonic acids,[21] reactions up to the acid in Scheme 1 are thought to mimic physiological processes. In spite of much experimental data accumulated, the following mechanistic questions have so far remained unanswered.

(1) In Scheme 1, the step of $AAH^- + OH\cdot \rightarrow AA^{\cdot -} + H_2O$ appears to include the hydrogen atom transfer (HAT).[22,23] However, the hydroxyl radical is a strong electrophilic species,[24] and the reaction between AAH^- and $OH\cdot$ is thought to be primarily an electrophilic addition.

(2) The step, $AA^{\cdot -} \rightarrow DHA + e^-$, appears to be an oxidation by one-electron loss. It is not clear how the step is described by geometric changes.

(3) How many elementary processes are involved in two hydrolyses, $DHA + H_2O \rightarrow BH$ and $DHA + H_2O \rightarrow DKG$? Is the hemiketal involved in the degradation channel?

(4) The step, $DKG + H_2O_2 \rightarrow THDH + H_2O$, is clearly a radical reaction; H_2O_2 should work as $2OH\cdot$ by the catalytic cupric sulfate[16] to break the C(5)-H covalent bond of DKG. On the other hand, in the reaction of $DKG + H_2O_2 \rightarrow$ threonic acid, apparently the $OH\cdot$ radical cannot participate in it. This is because the -C(3)(=O)-C(2)(=O)-C(1)(=O)OH moiety of DKG is very electrophilic and is not reactive toward the electrophilic $OH\cdot$ radical.

(5) The route from DKG to the two pentonic acids apparently consists of H_2O addition and CO_2 elimination. There are two questions. The first question is why the two epimers are generated in this process. The second is how the new C-H bond is formed at the α position of the carboxylic group.

In order to elucidate these issues, DFT calculations of reaction paths were carried out. While there are some theoretical studies of AAH_2 and the related species,[25] those of reaction paths including water molecules have not been reported. The condition used here is that one AAH_2 molecule is exposed to OH· radicals in the reaction AAH_2 → threonic and pentonic acids. Hydrogen bonds in the aqueous media would have a key role on the reaction mechanism, and the role was examined carefully in models including twelve water molecules.

2. Method of calculations

The reacting systems were investigated by density functional theory calculations. The B3LYP method[26,27] was used. The basis sets employed were 6-31G(d) for all species. Geometry optimizations and subsequent vibrational analyses were carried out including the polarizable continuum model (PCM) solvent effect (solvent=water).[28,29,30] Transition states (TSs) were sought first by partial optimizations at bond interchange regions. Second, by the use of Hessian matrices TS geometries were optimized. They were characterized by vibrational analysis, to confirm whether the geometries obtained had a single imaginary frequency ($\nu^{\ddagger}$). From TSs, reaction paths were traced by the intrinsic reaction coordinate (IRC) method[31,32] to obtain the energy-minimum geometries. Energy changes during the elementary reaction changes were computed from the sum of electronic and zero-point vibrational energies, "Et + ZPE". Free-energy changes were also calculated. TS geometries were re-optimized by a higher level computational method [M06-2X[33]/6-311+G** SCRF = (PCM, solvent=water)] to verify the reliability of the B3LYP/6-31G* SCRF = (PCM, solvent=water) calculations. Since TS6 in Figure 3 and TS18 in Figure 7 could not be obtained by this method, these were optimized at the B3LYP/6-311+G** SCRF=PCM level only. All the calculations were carried out using the GAUSSIAN 09 program package.[34] The computations were performed at the Research Center

for Computational Science, Okazaki, Japan.

3. Results and discussion

(3-1) From AAH_2 to $AA\cdot^-$ in the route [I]

Scheme 2 shows a reaction model, where AAH_2, $OH\cdot$ and $(H_2O)_{12}$ molecules are included. The water cluster is needed to trace the ionization process, $AAH_2 + (H_2O)_{12} \rightarrow AAH^- + H_3O^+(H_2O)_{11}$. While the inclusion of more than twelve water molecules to stabilize the oxonium ion is desirable, it complicates considerably the identification of the transition states. The molecular formula of the model in Scheme 2 is $C_6H_{33}O_{19}$. Other reacting systems were constructed uniformly to have nineteen oxygen atoms (e.g., $C_6H_{31}O_{19}^+$ in TS20 of Figure 8).

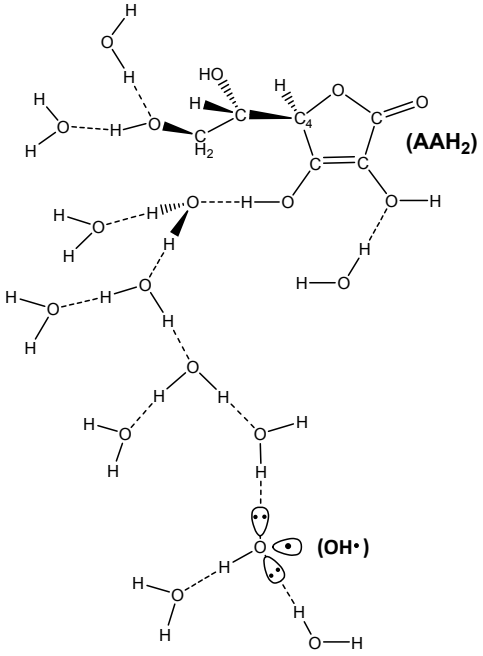

Scheme 2. The reaction model composed of L-ascorbic acid (AAH_2), hydroxyl radical and $(H_2O)_{12}$ to trace elementary steps in the route [I] of Scheme 1.

By the use of the model in Scheme 2, reaction paths were investigated. Figure 1 shows the geometries of the transition states (TSs) along the reaction paths. Those of the precursor [AAH_2 + OH radical + $(H_2O)_{12}$] and intermediates are given in Cartesian coordinates in the Supplementary Information.

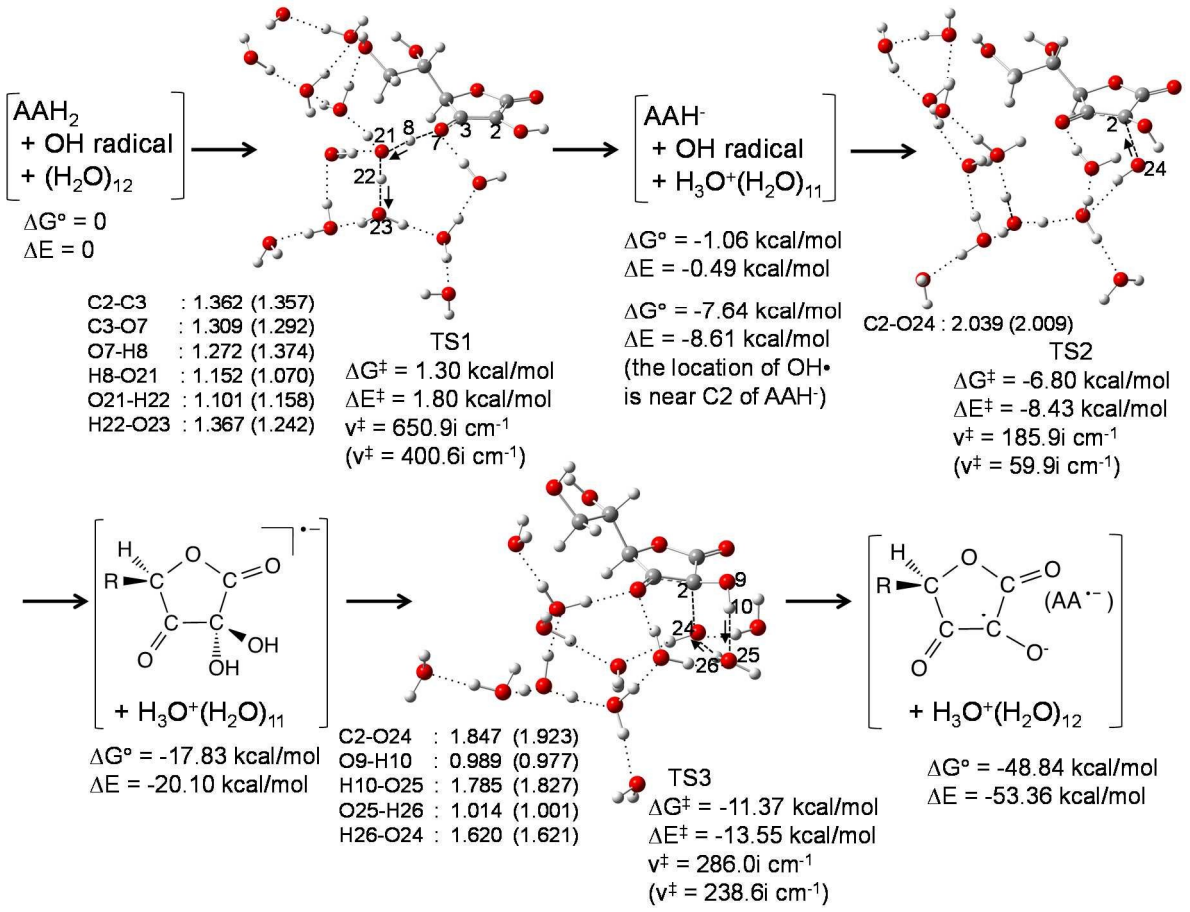

Figure 1. TS geometries along paths of the route [I]. ΔE is the relative energy in kcal/mol of electronic and vibrational ones, and ΔG is the relative Gibbs free energy (T = 298.15 K and P = 1 atm). Cartesian coordinates of TSs, precursor and intermediates are given in Supplementary Information. The substituent R- is $HOCH_2$-CH(OH)-. Distances (in Angstrom) and sole imaginary frequencies ($\nu^{\ddagger}$s) of TSs without and with parentheses are those obtained with B3LYP/6-31G* SCRF=PCM and M06-2X/6-311+G** SCRF=PCM, respectively.

TS1 is for the ionization with a very small activation energy (= +1.80 kcal/mol). After TS1, AAH^- and H_3O^+ are formed. The ion-pair system has almost the same stability (ΔE = -0.49 kcal/mol) as the precursor. The anion AAH^- may be subject to the electrophilic attack by the OH radical. The attacking position was predicted by the shape of HOMO (the highest occupied molecular orbital) of AAH^- shown in Figure 2(a).

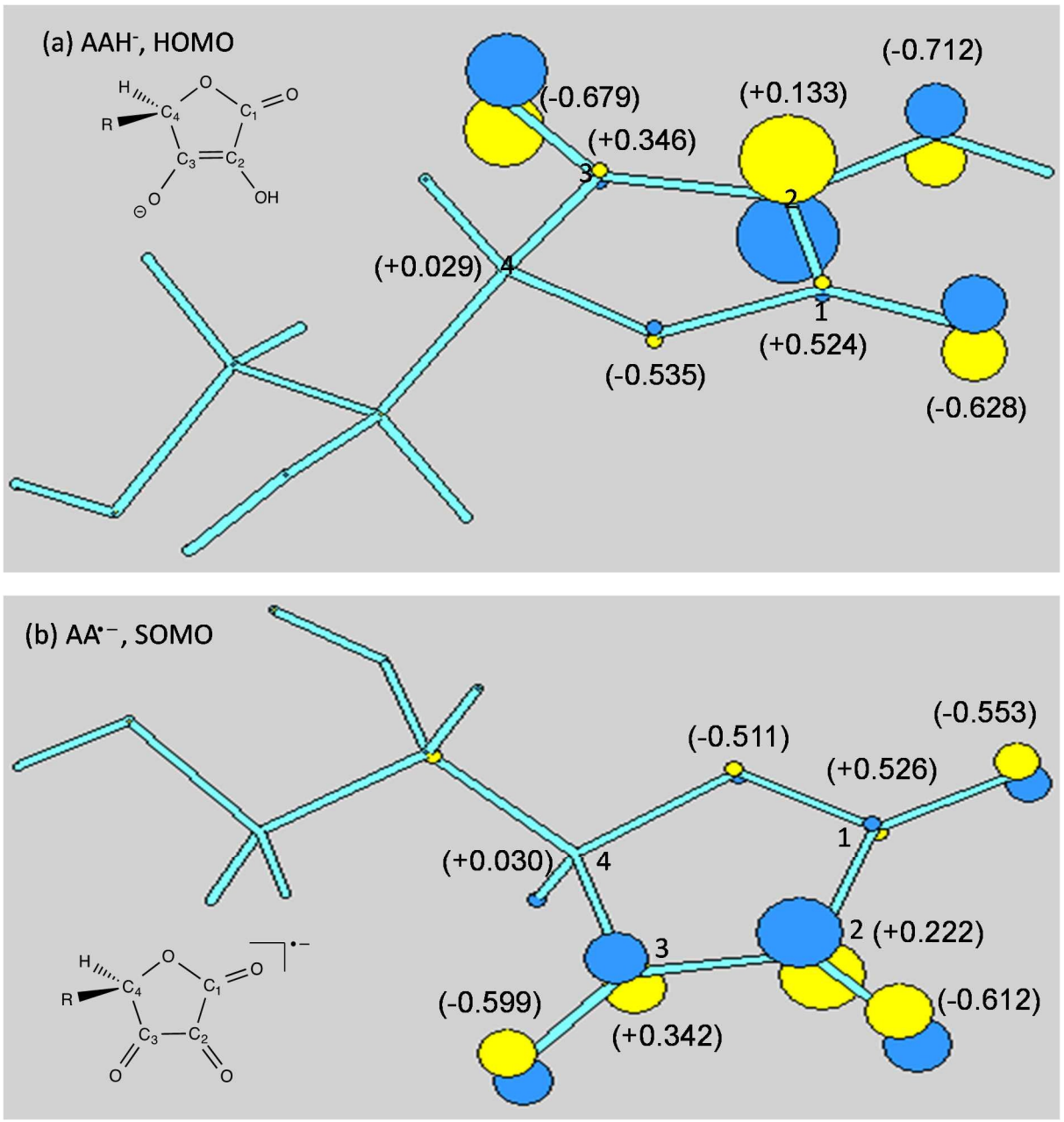

Figure 2. Frontier orbitals, HOMO, and SOMO in the radical species. (a) HOMO of AAH^-, (b) SOMO of $AA^{\cdot -}$. Values in parentheses are Mulliken electronic charges.

When the radical was located on C2 with the largest HOMO lobe,‡ a stable intermediate (ΔE = -8.61 kcal/mol) with the HO·····C2 distance 2.231 Å was obtained. From it, the electrophilic addition TS (TS2) is brought about to form the adduct anion radical. This radical is stable with ΔE = -20.10 kcal/mol. Its geminal two hydroxyl groups undergo the H_2O elimination with one auxiliary water molecule at TS3. It has a small activation energy +6.65

kcal/mol (-13.55-(-20.10)). The resultant anion radical is $AA^{\cdot -}$ with a significantly large exothermic energy, -53.36 kcal/mol. This energy indicates that this species can be detected in ESR experiments.[10] The anion radical is even more stable than the neutral one AAH· (the species Ia in Ref. 10) as shown in Figure S2. The conversion from AAH^- to $AA^{\cdot -}$ is depicted in Scheme 3(A). The direct hydrogen-loss path, $AAH^- + OH\cdot \rightarrow AA^{\cdot -} + H_2O$, could not be obtained.

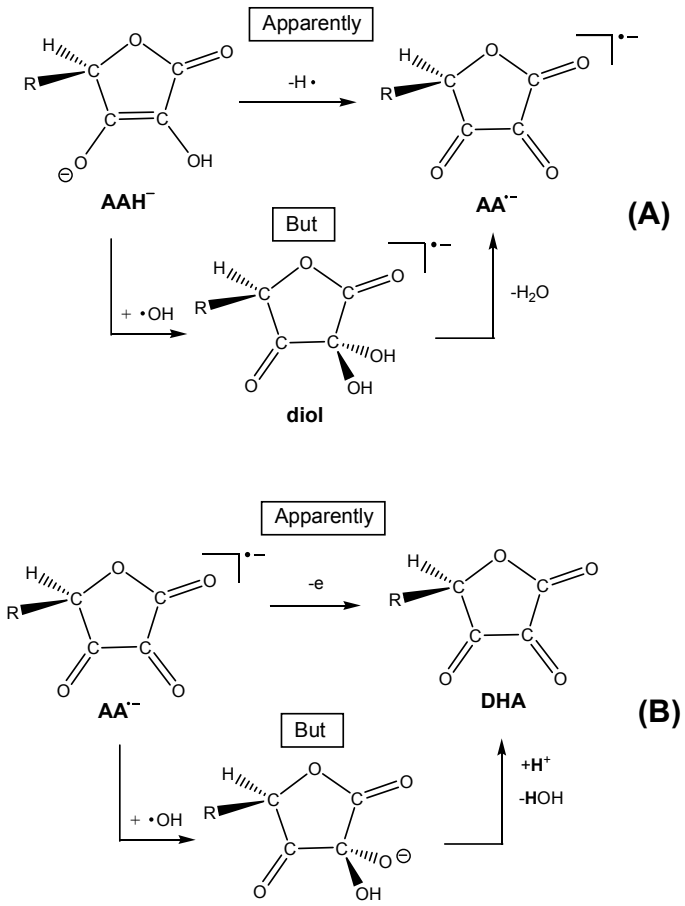

Scheme 3. Two stepwise processes (A) and (B) including OH radical adducts. The substituent R- is $HOCH_2$-CH(OH)-.

(3-2) From $AA^{\cdot -}$ + OH· to BH in the route [II]

While the ascorbate anion radical ($AA^{\cdot -}$) is a very stable species, it will be subject to the electrophilic attack of the second OH radical. The attacking position may be predicted by the SOMO (singly occupied molecular orbital) shape of $AA^{\cdot -}$, which is shown in Figure 2(b).

At C2, SOMO has the largest lobe, and the radical-radical recombination therefore occurs at this site. The ($AA\cdot^-$ and $OH\cdot$) adduct with $H_3O^+(H_2O)_{11}$ is taken to be the starting point of the route [II] (and [III]). The adduct undergoes the H_2O elimination at TS4 leading to the dehydroascorbic acid (DHA) (Figure 3). Conversion from $AA\cdot^-$ to DHA is illustrated in Scheme 3(B). The activation energy of the dehydration is small, $\Delta E^{\ddagger}$ = +8.52 kcal/mol, and DHA is slightly more stable (ΔE = -2.16 kcal/mol) than the preceding adduct.

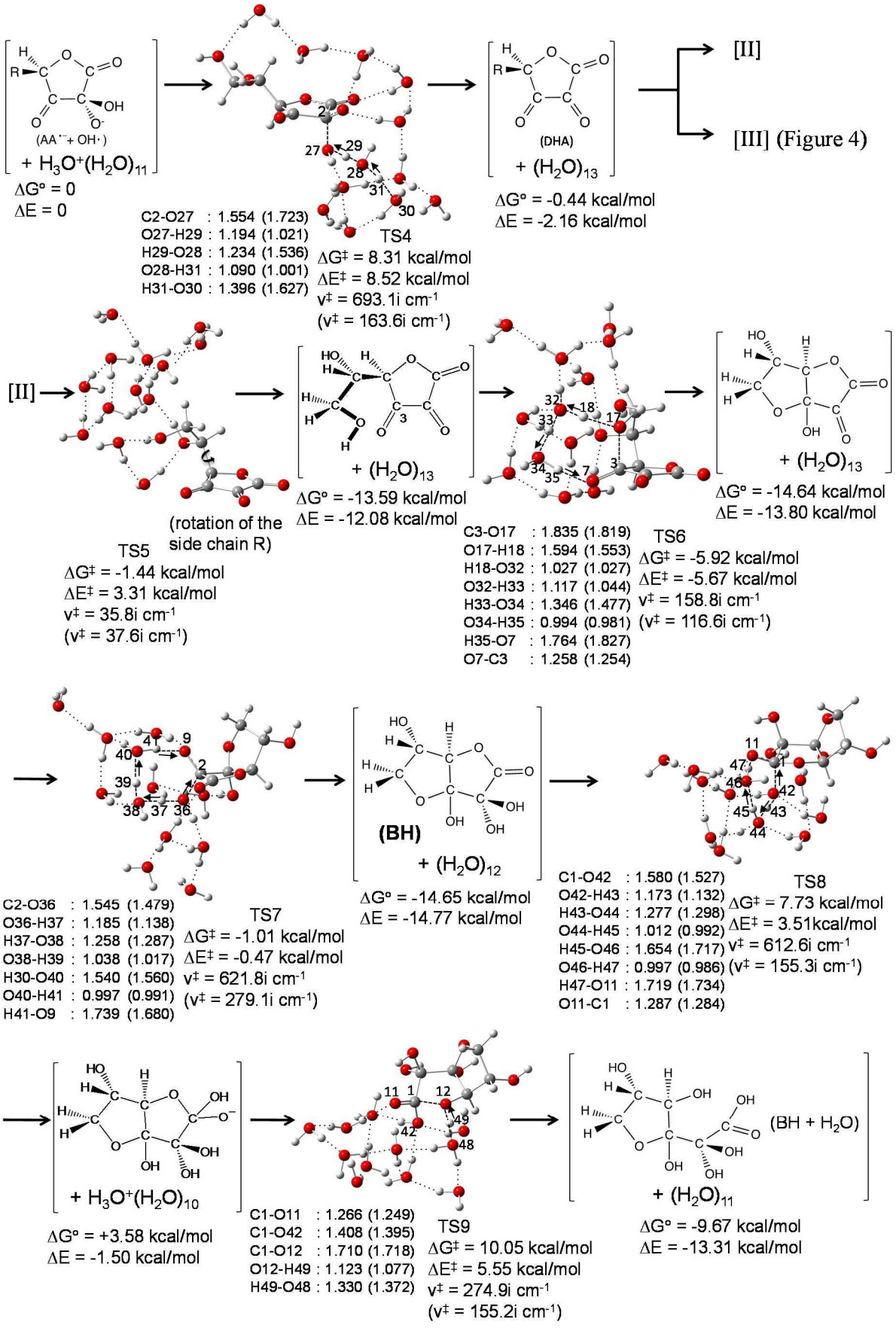

Figure 3. TS geometries at formation of DHA and along paths of the route [II].

In DHA, the five membered ring is electrophilic due to three carbonyl groups, and the terminal hydroxyl group of the side chain (R) moves toward the ring via the internal rotation (TS5). After TS5, a DHA isomer with the C3·····OH (the terminal OH) distance 2.528 Å. A through-space interaction (attraction) is involved in the isomer. Ring closure occurs via proton transfers with two water molecules (TS6). The participation of the water dimer in the ring closure was calculated to be likely on the basis of comparison of activation energies in a model reaction, DHA + $(H_2O)_n$ → 2,6-dioxa-5,8-dihydroxy-bicyclo[3.3.0]octan-3,4-dione (BH) + $(H_2O)_n$, n=0, 1, 2 and 3 as shown in Figure S3. A bicyclic intermediate with the exothermic energy -13.80 kca/mol is formed, which reacts with the water trimer (TS7) to arrive at BH. While BH is an identified compound,[14] its lactone ring might undergo the cleavage to afford a carboxylic acid. In order to check the cleavage, further processes were traced. The two transition states TS8 and TS9 were identified, which are involved in the formation of the carboxylic acid ("BH+H_2O" at the end of Figure 3). However, BH+H_2O is less stable than BH, and BH is the end of the route [II]. Thus, while BH is a stable and probable intermediate, it does not undergo the degradation and would be converted back to DHA to take the route [III].

(3-3) From DHA to DKG and a CO_2-eliminated anion radical in the route [III]

The dehydroascorbic acid (DHA) is hydrolyzed to the diketogulonic acid (DKG) via TS10 and TS11 as shown in Figure 4. The bond interchanges (mainly O-H····O → O····H-O) involved in these two TSs are sketched in Scheme 4.

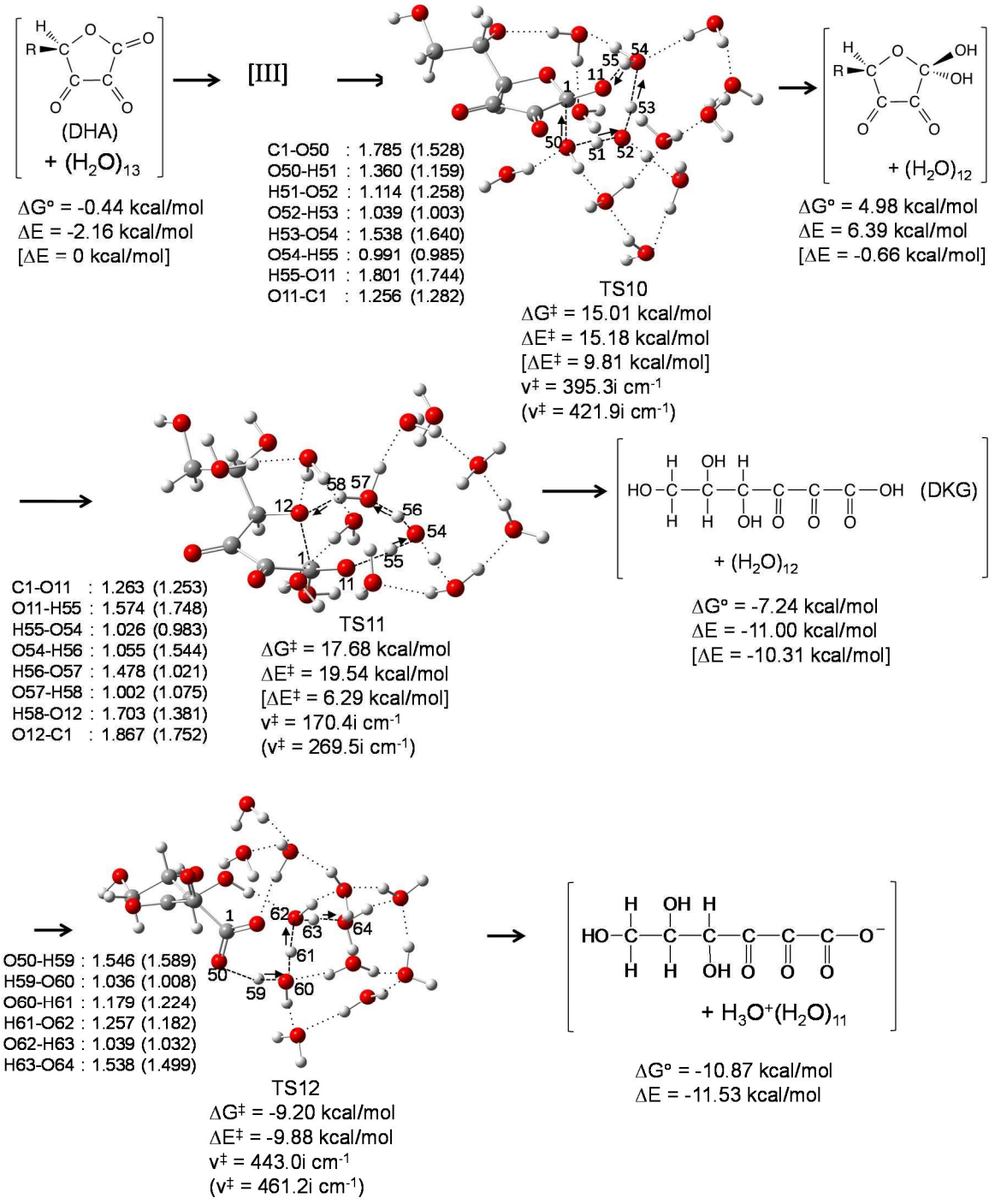

Figure 4. TS geometries along paths of DHA → the conjugate base of DKG in the route [III]. ΔE values in square brackets are of the acid-catalyzed reactions shown in Figure S4.

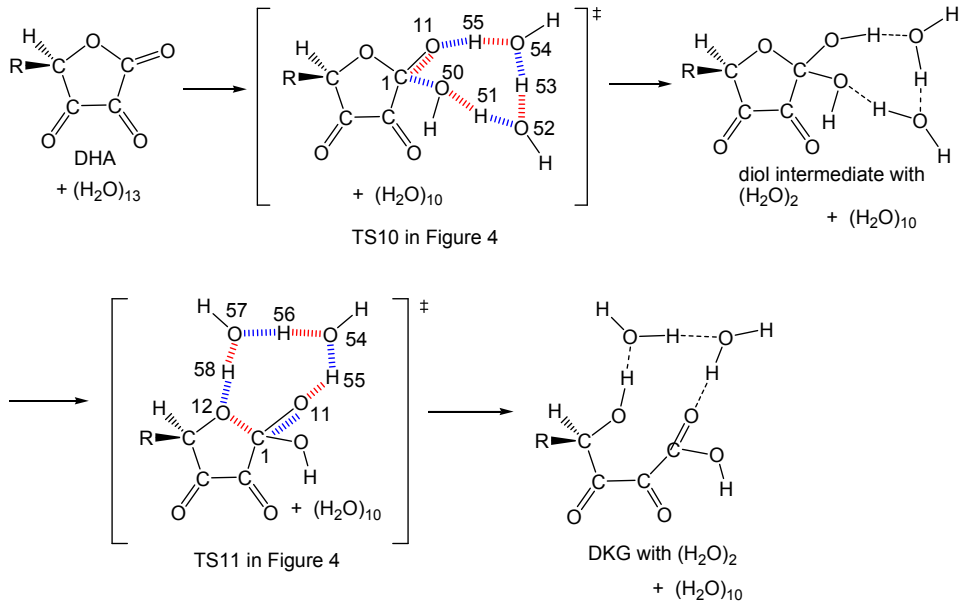

Scheme 4. The ring-opening reaction, DHA → DKG, promoted by proton transfers through O···H···O hydrogen bonds. At TSs, red broken lines stand for covalent bonds cleaved and blue ones do for those formed.

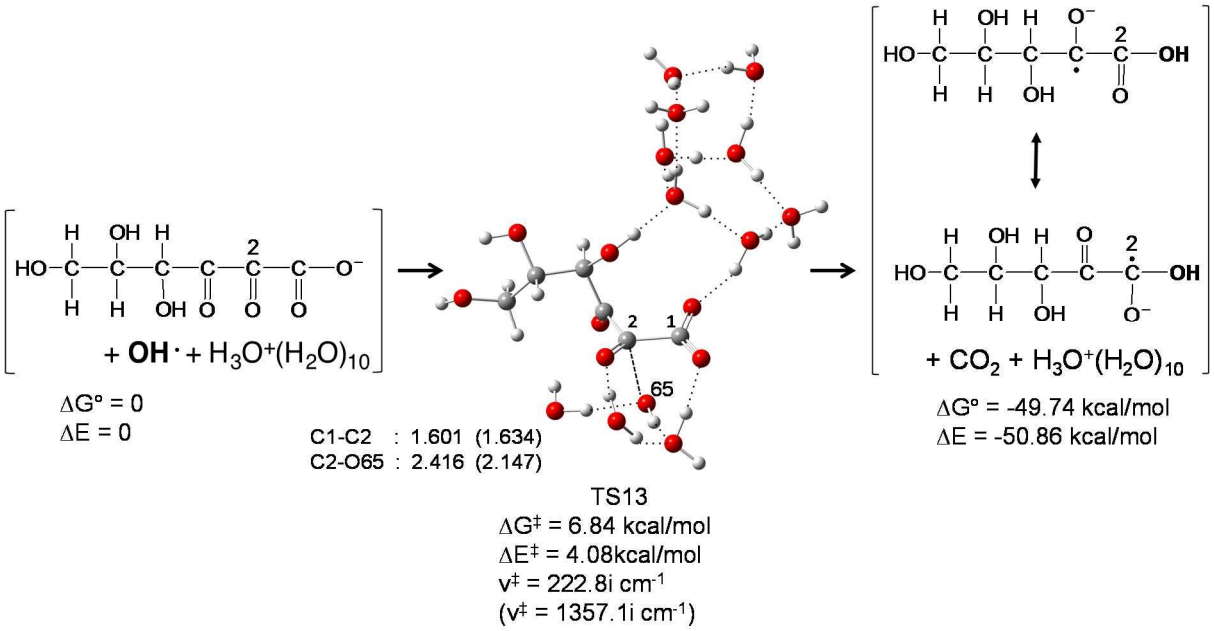

Figure 5. A CO_2 extrusion path starting from the conjugate base of DKG and **OH**·.

Between TS10 and TS11, an unstable intermediate with a tetrahedral carbon atom (ΔE= +6.39 kcal/mol) is formed. The activation energy of TS11, $\Delta E^{\ddagger}$ = +19.54 kcal/mol, is too large for the

neutral ester hydrolysis to occur readily. Since a proton is released during the ionization of $AAH_2 \rightarrow AAH^- + H^+$, an acid catalyzed hydrolysis is conceivable. Figure S4 exhibits the acid-promoted (DHA → DKG) reaction. In the catalytic process, the activation energies are small [$\Delta E^{\ddagger}$= +9.81 kcal/mol (TS10)] and [$\Delta E^{\ddagger}$ = +6.29 kcal/mol (TS11)]. Both uncatalyzed and catalyzed ring-opening reactions were calculated to occur through proton transfers with two or three water molecules. DKG is ionized to the carboxylate via TS12 with a very small activation energy, 1.12 (-9.88-(-11.00)) kcal/mol.

The carboxylate, *i.e.*, the conjugate base of DKG, HO-CH_2-CH(OH)-CH(OH)-C(=O)-C(=O)-COO^- may be subject to the electrophilic attack of OH·. Figure S1(a) shows the shape of HOMO-1 of the carboxylate, where HOMO is the π MO on the two carboxyl oxygen atoms. Besides the in-plane lobes on the carboxyl oxygen atoms, there is a lobe at the carbonyl carbon (C2). The most favorable attack site for OH· will therefore be C2. Then, the carbon will be bound to the attacking OH·. According to the FMO prediction, the (O=)C2·····OH· approaching path was sought, and TS13 was obtained, which is shown in Figure 5. After the formation of TS13, a bond is formed between C2 and O(65)H. This process leads to the evolution of CO_2. It was found that the α-keto carboxylate undergoes the OH· electrophilic addition, which leads to the decarboxylation, *i.e.*, degradation. After TS13, an anion radical HO-CH_2-CH(OH)-CH(OH)-C·(-O^-)-COOH with a large exothermic energy ΔE = -50.86 kcal/mol is formed.

The shape of the SOMO of the anion radical is shown in Figure S1(b). As expected, the largest lobe of the SOMO is at C1 (adjacent to the carboxyl group). At the carbon, the radical-radical recombination with the fourth **OH**· takes place readily. Subsequently, the adduct HO-CH_2-CH(OH)-CH(OH)-C(**OH**)(-O^-)-COOH proceeds through a dehydration path similar to TS4 ($AA^{\cdot -}$ + OH· → DHA in Figure 3). This leads to the formation of an α-keto carboxylic acid HO-CH_2-CH(OH)-CH(OH)-C(=O)-COOH (L-threo-2-pentulsonic acid in Scheme 1). Following this step, the ionization of this species leading to HO-CH_2-CH(OH)-CH(OH)-C(=O)-COO^-, the fifth OH· addition with the CO_2 elimination, the sixth OH· addition and the H_2O elimination give the threonic acid in a way similar to the conversion of DKG → pentulsonic acid. Threonic acid HO-CH_2-CH(OH)-CH(OH)-COOH is the final product,

because no further α carbonyl groups are available for OH· addition.

(3-4) Formation of two pentonic acids

In Figure 5, the product is an anion radical HO-CH_2-CH(OH)-CH(OH)-C·(O^-)-COOH. This anion radical may be subject either to the OH· addition via radical-radical recombination to give 2-pentulsonic acid or to the neutralization. These reactions are shown in Figure 6. In this sub-section, the latter process is examined. The alkoxide-ion oxygen O(5) is protonated at TS14, and the neutral radical HO-CH_2-CH(OH)-CH(OH)-C·(OH)-COOH is produced. The radical may capture a hydrogen atom from a C-H bond of the other coexisting species. Here, threonic acid is regarded as the starting species, and the hydrogen migration is shown as TS15. The resulting radical HO-CH_2-CH(OH)-C·(OH)-COOH (after TS15) may be the source of the further degradation to product, glyceric acid and aldehyde (Ref. 1) as shown in Figure S5.

Through the hydogen-atom capture of TS15, L-lyxonic acid (*S* configuration at C2) is generated. The H. abstraction by threonic acid is also possible in the direction of the planar radical center opposite to that shown in TS15. The possibility leads to the epimer, i.e., L-xylonic acid (*R* configuration at C2). Figure 6 shows how the C=O bond is converted to CH(OH) moiety at the fourth atom (from the left) of DKG.

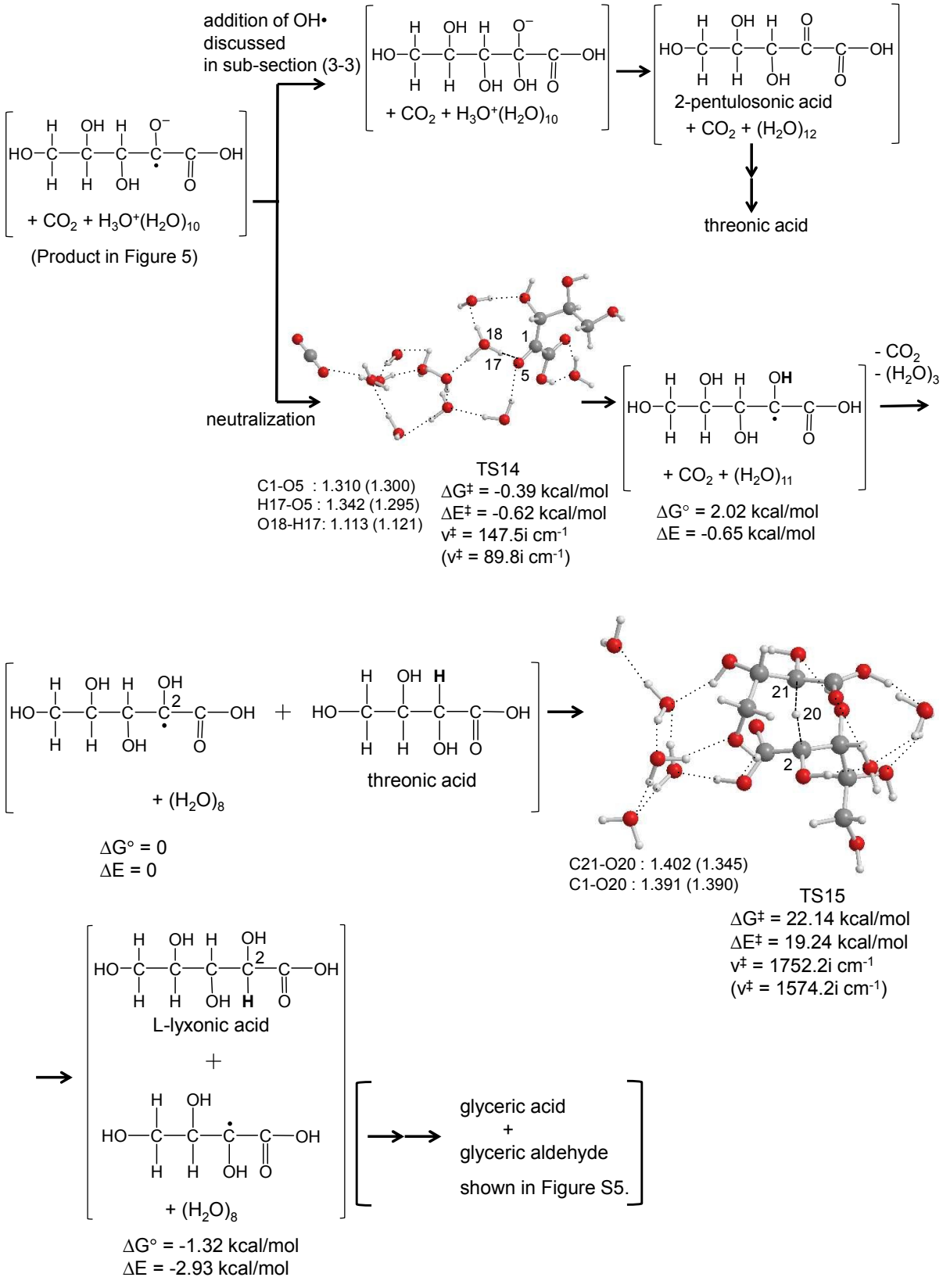

Figure 6. Formation of L-lyxonic acid starting from the anion radical given in Figure 5. All the TS geometries are taken to have 19 oxygen atoms. Therefore, $CO_2(H_2O)_3$ is subtracted at the

hydrogen abstraction step, resulting in the molecular formula $C_9H_{33}O_{19}$ of TS15 and its precursor.

(3-5) Formation of threonic acid and oxalic acid

In subsection (3-3) the reaction of the conjugated base of DKG with the OH· radical has been examined, in which the substrate is a nucleophile and reacts with the strong OH· electrophile. In order for DKG to react without ionization, the OH· radical needs to be transformed to the other species. The most likely transformation is the radical recombination $2OH· \rightarrow HO\text{-}OH$. The combination of DKG and HO-OH might give a second degradation. In fact, Deutsch investigated the reaction of DKG and HO-OH as described in the Introduction and shown in Scheme 1.[16,17] A reaction model composed of DKG, H_2O_2 and $(H_2O)_{10}$ was examined. The calculated paths are shown in Figure 7.

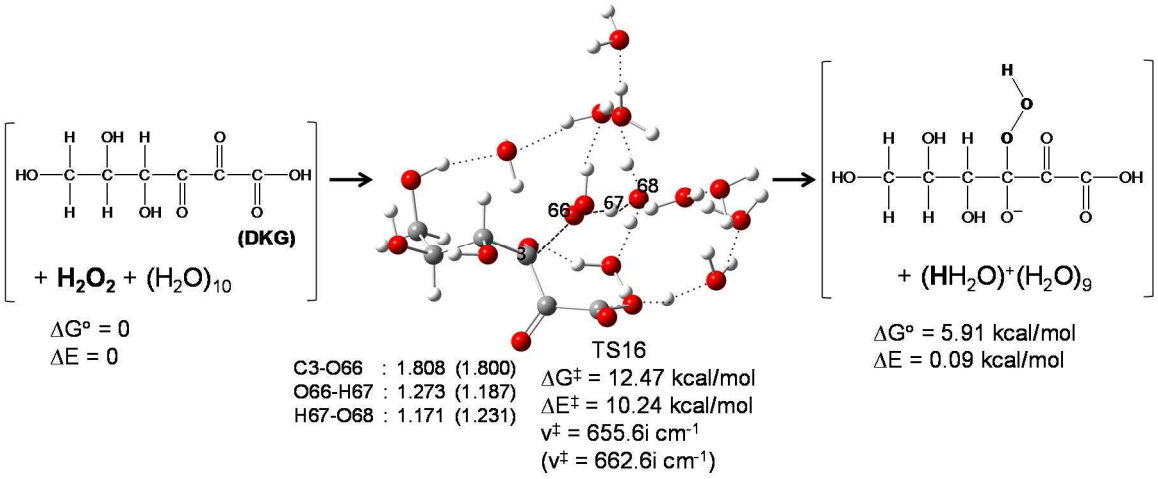

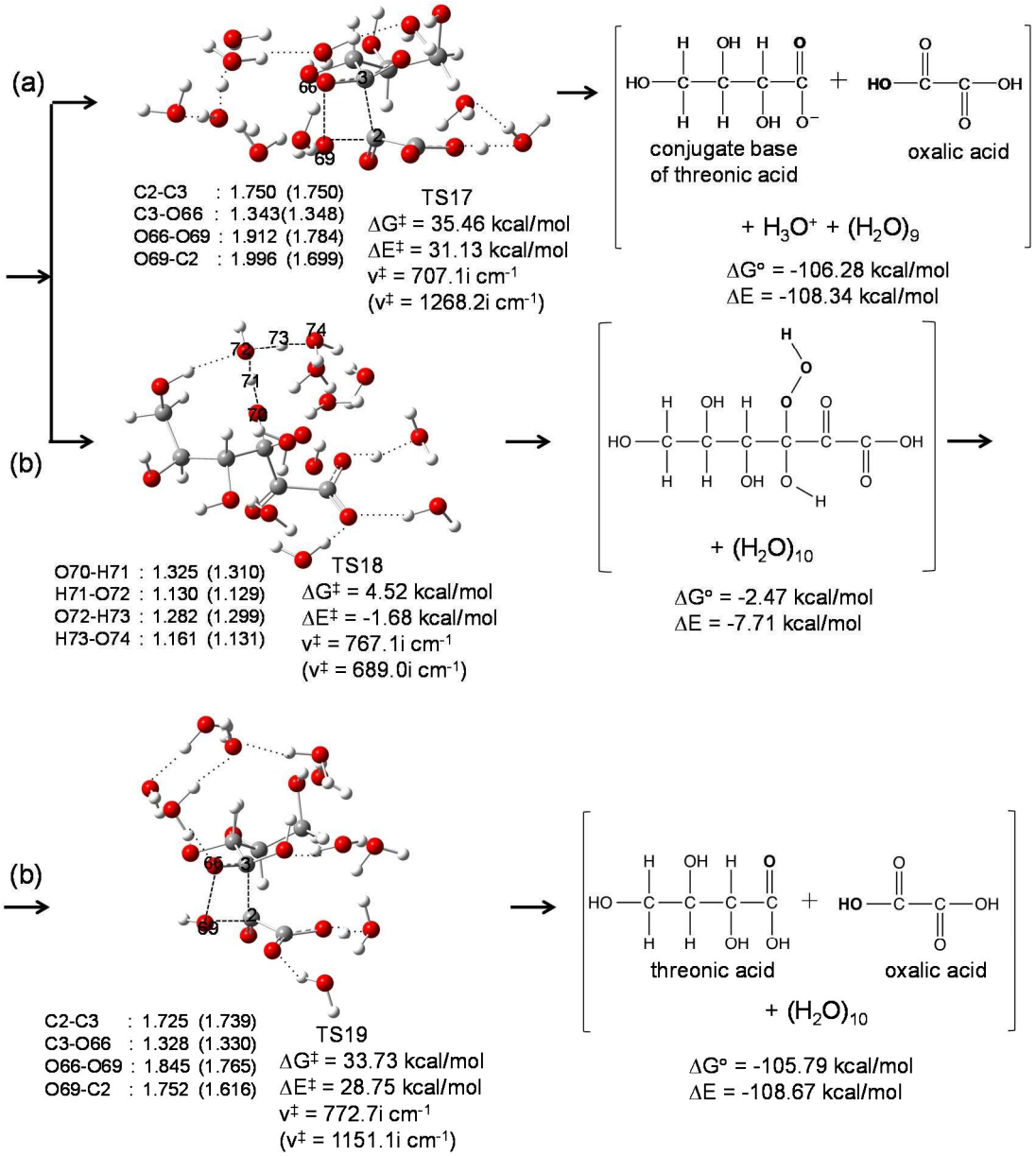

Figure 7. Paths of a reaction of DKG (diketogulonic acid) and H_2O_2, leading either to a pair of the conjugate base of threonic acid and oxalic acid (a) or to two acids (b).

The first step was found to be a nucleophilic attack of OOH^- concomitant with the deprotonation of HO-OH at TS16. This step is similar to the first one of the Dakin oxidation[35] in *ortho*-hydroxybenzaldehyde, H_2O_2 and NaOH where the OOH^- adds to the carbonyl carbon forming an intermediate with a tetrahedral carbon atom. An ion pair intermediate with the C-O-O-H moiety is formed after TS16. From the intermediate, two channels (a) and (b) were found. In TS17 of (a), the OH migration and C-C cleavage occur at the same time. After TS17, an ion pair composed of the conjugate base of threonic acid and oxalic acid is generated. In TS18 of (b), the alkoxide oxygen is protonated, which leads to an intermediate containing the C(OH)(OOH) moiety. Subsequently, OH migration and C-C cleavage take place at TS19. The product contains two acids. While the paths in Figure 7 appear to be likely, the activation energies of TS17 ($\Delta E^{\ddagger}$ = +31.13 kcal/mol) and TS19 ($\Delta E^{\ddagger}$ = +28.75) are large. This may disfavor this process under kinetic control conditions.

Since DKG is ionized readily as shown in TS12 (Fig. 4), the proton catalyst might contribute to lower the activation energy. Figure 8 exhibits a proton containing reaction starting from the neutral intermediate between TS18 and TS19 ($HOCH_2$-CH(OH)-CH(OH)-C(OH)(OOH)-C(=O)-COOH in Fig. 7). This intermediate evolves through TS20 to generate a geminal -OH pair. Then, the C-C bond may be cleaved readily at TS21, which leads to two acids. The activation energy $\Delta E^{\ddagger}$ of TS21 is +15.56 kcal/mol, which is much smaller than the corresponding one, +36.46 (= +28.75(TS19)-(-7.71)) kcal/mol in Figure 7.

Thus, the simultaneous formation of threonic acid and oxalic acid is brought about by the combination of the electrophile DKG and the nucleophile HO-OH.

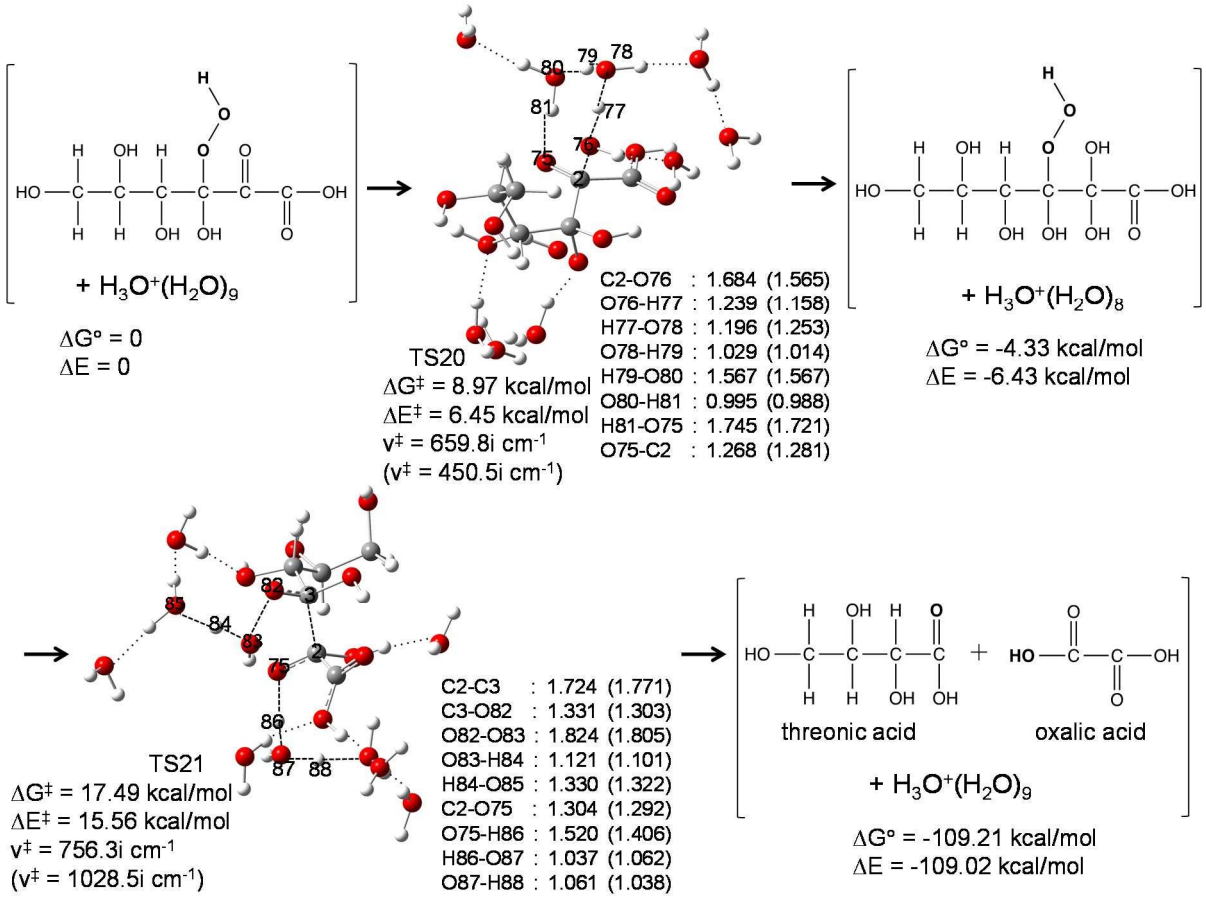

Figure 8. An acid-catalyzed conversion of the HO-CH_2-CH(OH)-CH(OH)-C(OH)(OOH)-C(=O)-COOH intermediate to the product of two acids.

It is noteworthy that the reaction energies of the three products in Figures 7 and 8 are -108~ -109 kcal/mol. These significantly large exothermic energies indicate that the reaction from DKG to threonic and oxalic acids occurs under thermodynamic control.

4. Concluding remarks

In this work, DFT calculations were performed to investigate the reaction paths of L-ascorbic acid (AAH_2), hydroxyl radical and water clusters. FMO analyses were also made to identify the OH· addition site at the substrate. Calculated elementary steps along with probable ones were designated [a], [b], [c].... and [p] and are shown in Scheme 5(A), (B) and (C). Routes [I], [II] or [III] are the same as those in Scheme 1.

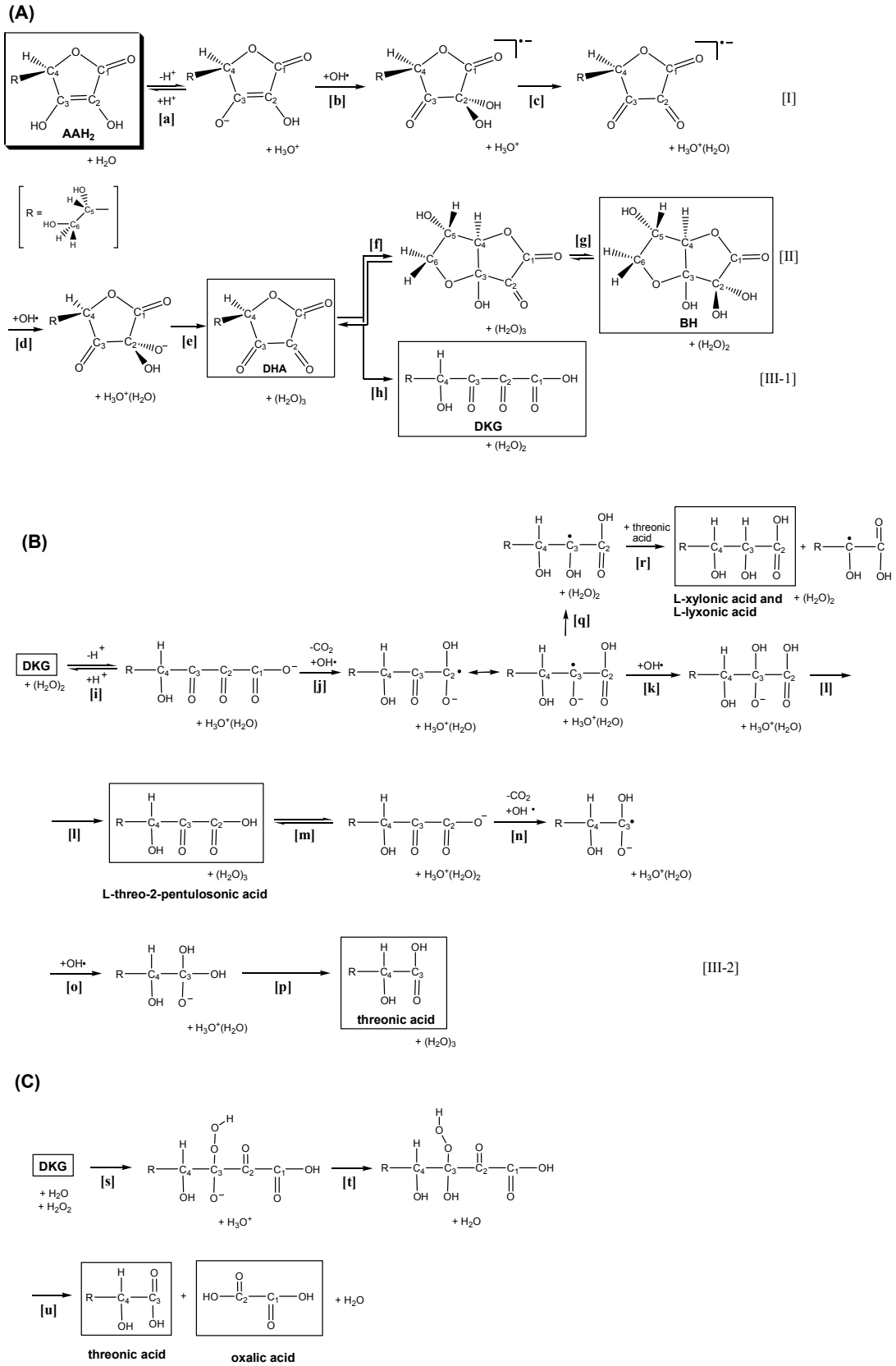

Scheme 5. Summary of the present calculated results and the proposed routes from AAH_2 to

species in boxes. The numbering of carbon atoms for AAH_2 is retained in all structural formulae. Each step is explained in Supplementary Information.

In the Introduction, five questions have been raised, and they may be answered on the basis of Scheme 5.

(1) While the reaction of $AAH^- + OH\cdot \rightarrow AA\cdot^- + H_2O$ in the route [I] appears to occur via the HAT mechanism, it consists of an OH· addition (the step [b]) followed by dehydration (the step [c]).

(2) The oxidation, $AA\cdot^- \rightarrow DHA + e^-$ in the route [I], consists of a radical-radical recombination (the step [d]) and the subsequent dehydration (the step [e]).

(3) From DHA, the ring closure (the step [f]) and the subsequent hydration (the step [g]) lead to a bicyclic hemiketal intermediate (BH). The ring opening of BH generates an unstable carboxylic acid. Then, BH is not involved in the degradation channel. The ring opening process of DHA → DKG in the step [h] is an acid catalyzed ester hydrolysis.

(4) DKG and other α-keto carboxylic acids are ionized to become carboxylates, *i.e.*, nucleophiles, which are subject to the addition of OH· leading to the CO_2 elimination (degradation).

(5) The neutral radical R-CH(OH)-C·(OH)-COOH has a planar reaction center, which may capture hydrogen atom from two out-of-planar directions leading to two pentonic acids (epimers).

DKG reacts with the hydroxyl radical so as to form the threonic acid in two ways. One is formation of the anionic site subject to the electrophilic OH· addition in Scheme 5**(B)**. The other is the radical-radical recombination of two OH· to give the nucleophile HO_2^- where the substrate DKG is an electrophile. Both routes are consistent with the dual appearance of the threonic acid in Scheme 1 of Ref. 19.

As a whole, the oxidation and degradation of vitamin C therefore occur via a donor (AAH_2) - acceptor (OH·) reaction pathway.

Footnotes

† Electronic supplementary information (ESI) available: Figures S1-6, auxiliary explanations to Schemes 1 and 5, and Cartesian coordinates of the optimized geometries and energies.

‡ In Figure 2(a), there is also a lobe on the anionic oxygen bonded to C(3). The lobe might be subject to the OH· addition. To check the possibility, an adduct geometry with the C(3)-O-O-H moiety was optimized, where the O-O bond distance was assumed to be 1.47 Å. However, the optimization leads to a different geometry with the C(3)-O·····H-O moiety. The result may be interpreted in terms of the kinetic preference (HOMO extension) and the thermodynamic instability of the adduct for the OH· attack onto the anionic oxygen.

References

(1) M. Smuda and M. A. Glomb, *Angew. Chem. Int. Ed*., 2013, **52**, 4887‑4891.

(2) A. Szent-Gyorgyi, *Biochem. J.*, 1928, **22**, 1387-1409.

(3) J. L. Svirbely and A. Szent-Gyorgyi, *Nature*, 1932, **129**, 576.

(4) A. Szent-Gyorgyi and W. N. Haworth, *Nature*, 1933, **131**, 24.

(5) R. W. Herbert, E. L. Hirst, E. G. V. Percival, R. J. W. Reynolds and F. Smith, *J. Chem. Soc*., 1933, 1270-1290.

(6) J. Hvoslef, *Acta Crystallogr. Sect. B*, 1968, **24**, 23-35.

(7) R. S. Reid, *J. Chem. Educ*., 1989, **66**, 344-345.

(8) M. B. Davies, J. Austin and D. A. Partridge, "Vitamin C: its chemistry and biochemistry", Royal Society of Chemistry, Cambridge, 1991, pp 3-15.

(9) I. Yamazaki, H. S. Mason and L. H. Piette, *J. Biol. Chem*., 1960, **235**, 2444-2449.

(10) G. P. Laroff, R. W. Fessenden and R. H. Schuler, *J. Am. Chem. Soc*., 1972, **94**, 9062-9073.

(11) G. R. Buettner and B. A. Jurkiewicz, *Free Radical Biol. Med*., 1993, **14**, 49-55.

(12) A. Bendich, L. J. Machlin, O. Scandurra, G. W. Burton and D. D. M. Wayner, *Adv. Free Radical Biol. Med*., 1986, **2**, 419-444.

(13) G. R. Buettner and B. A. Jurkiewics, *Free Radical Biol. Med*., 1993, **14**, 49-55.

(14) L. W. Donner and K. B. Hicks, in "Methods in Enzymology", (F. Chytil and D. B. McCormick, Eds.), 1986, **122**, pp. 3-10, Academic Press, New York.

(15) J. C. Deutsch and C. R. Santhosh-Kumar, *J. Chromatogr. A*, 1996, **724**, 271-278.

(16) J. C. Deutsch, C. R. Santhosh-Kumar, K. L. Hassell and J. F. Kolhouse, *Anal. Chem*., 1994, **66**, 345-350.

(17) (a) J. C. Deutsch, *Anal. Biochem*., 1998, **255**, 1-7. (b) J. C. Deutsch, *Anal. Biochem*., 1998, **260**, 223-229.

(18) S. Englard and S. Seifter, "The Biochemical Functions of Ascorbic Acid". Annual Review of Nutrition, 1986, **6**, 365-406.

(19) K. Niemela, *J. Chromatogr.*, 1987, **399**, 235-243.

(20) J. Kanfer, G. Ashwell and J. J. Burns, *J. Biol. Chem.*, 1960, **235**, 2518-2521.

(21) H. S. Isbell and H. L. Frush, *Carbohydrate Research*, 1979, **72**, 301-304.

(22) D. Njus, V. Jalukar, J. Zu and P. M. Kelley, *Am. J. Clin. Nutr*., 1991, **284**, 1179-1183.

(23) Y.-N. Wang, K.-C. Lau, W. W. Y. Lam, W.-L. Man, C.-F. Leung and T.-C. Lau, *Inorg. Chem*., 2009, **48**, 400-406.

(24) H. Marusawa, K. Ichikawa, N. Narita, H. Murakami, K. Ito and T. Tezuka, *Bioorg. Med. Chem*., 2002, **10**, 2283-2290.

(25) (a) P. Li, Z. Shen, W. Wang, Z. Ma, S. Bi, H. Suna and Y. Bu, *Phys. Chem. Chem. Phys*., 2010, **12**, 5256–5267. (b) R.-N. Zhao, Y. Yuan, F. Liu, J.-G. Han and L. Sheng, *Int. J. Quantum Chem*., 2013, **113**, 2220–2227. (c) Y.-N. Wang, K.-C. Lau, W. W. Y. Lam, W.-L. Man, C.-F. Leung and T.-C. Lau, *Inorg. Chem.*, 2009, **48**, 400–406. (d) R. N. Allen, M. K. Shukla, D. Reed and J. Leszczynski, *Int. J. Quantum Chem*., 2006, **106**, 2934–2943. (e) J. R. Juhasz, L. F. Pisterzi, D. M. Gasparro, D. R. P. Almeida and I. G. Csizmadia, *J. Mol. Struct*. (Theochem), 2003, **666–667**, 401–407. (f) M. A. Al-Laham, G. A. Petersson, and P. Haake, *J. Computational Chem.*, 1991, **12**, 113–118.

(26) A. D. Becke, *J. Chem. Phys*., 1993, **98**, 5648-5652.

(27) C. Lee, W. Yang and R. G. Parr, *Phys. Rev. B*, 1988, **37**, 785-789.

(28) E. Cances, B. Mennucci and J. Tomasi, *J. Chem. Phys*., 1997, **107**, 3032-3041.

(29) M. Cossi, V. Barone, B. Mennucci and J. Tomasi, *Chem. Phys. Lett*., 1998, **286**, 253-260.

(30) Mennucci, B.; Tomasi, J. *J. Chem. Phys*. **1997**, *106*, 5151-5158.

(31) K. Fukui, *J. Phys. Chem*., 1970, **74**, 4161-4163.

(32) C. Gonzalez and H. B. Schlegel, *J. Chem. Phys*., 1989, **90**, 2154-2161.

(33) (a) Y. Zhao and D. G. Truhlar, *Theor. Chem. Acc*., 2008, **120**, 215-241. (b) Y. Zhao and D. G. Truhlar, *Acc. Chem. Res*., 2008, **41***,* 157-167.

(34) Gaussian 09, Revision D.01, M. J. Frisch, G. W. Trucks, H. B. Schlegel, G. E. Scuseria, M. A. Robb, J. R. Cheeseman, G. Scalmani, V. Barone, B. Mennucci, G. A. Petersson, H. Nakatsuji, M. Caricato, X. Li, H. P. Hratchian, A. F. Izmaylov, J. Bloino, G. Zheng, J. L. Sonnenberg, M. Hada, M. Ehara, K. Toyota, R. Fukuda, J. Hasegawa, M. Ishida, T. Nakajima, Y. Honda, O. Kitao, H. Nakai, T. Vreven, J. A. Montgomery, Jr., J. E. Peralta, F. Ogliaro, M. Bearpark, J. J. Heyd, E. Brothers, K. N. Kudin, V. N. Staroverov, R. Kobayashi, J. Normand, K. Raghavachari, A. Rendell, J. C. Burant, S. S. Iyengar, J. Tomasi, M. Cossi, N. Rega, J. M. Millam, M. Klene, J. E. Knox, J. B. Cross, V. Bakken, C. Adamo, J. Jaramillo, R. Gomperts, R. E. Stratmann, O. Yazyev, A. J. Austin, R. Cammi, C. Pomelli, J. W. Ochterski, R. L. Martin, K. Morokuma, V. G. Zakrzewski, G. A. Voth, P. Salvador, J. J. Dannenberg, S. Dapprich, A. D. Daniels, Ö. Farkas, J. B. Foresman, J. V. Ortiz, J. Cioslowski, and D. J. Fox, Gaussian, Inc., Wallingford CT, 2009.

(35) (a) H. D. Dakin, *Am. Chem. J*., 1909, **42**, 477-498. (b) H. D. Dakin, *Org. Synth*., 1941, Coll. Vol. **1**, 149-153.